

SANDIA REPORT

SAND2012-1772

Unlimited Release

Printed March 2012

PV Output Smoothing with Energy Storage

Abraham Ellis and David Schoenwald

Prepared by
Sandia National Laboratories
Albuquerque, New Mexico 87185 and Livermore, California 94550

Sandia National Laboratories is a multi-program laboratory managed and operated by Sandia Corporation, a wholly owned subsidiary of Lockheed Martin Corporation, for the U.S. Department of Energy's National Nuclear Security Administration under contract DE-AC04-94AL85000.

Approved for public release; further dissemination unlimited.



Sandia National Laboratories

Issued by Sandia National Laboratories, operated for the United States Department of Energy by Sandia Corporation.

NOTICE: This report was prepared as an account of work sponsored by an agency of the United States Government. Neither the United States Government, nor any agency thereof, nor any of their employees, nor any of their contractors, subcontractors, or their employees, make any warranty, express or implied, or assume any legal liability or responsibility for the accuracy, completeness, or usefulness of any information, apparatus, product, or process disclosed, or represent that its use would not infringe privately owned rights. Reference herein to any specific commercial product, process, or service by trade name, trademark, manufacturer, or otherwise, does not necessarily constitute or imply its endorsement, recommendation, or favoring by the United States Government, any agency thereof, or any of their contractors or subcontractors. The views and opinions expressed herein do not necessarily state or reflect those of the United States Government, any agency thereof, or any of their contractors.

Printed in the United States of America. This report has been reproduced directly from the best available copy.

Available to DOE and DOE contractors from

U.S. Department of Energy
Office of Scientific and Technical Information
P.O. Box 62
Oak Ridge, TN 37831

Telephone: (865) 576-8401
Facsimile: (865) 576-5728
E-Mail: reports@adonis.osti.gov
Online ordering: <http://www.osti.gov/bridge>

Available to the public from

U.S. Department of Commerce
National Technical Information Service
5285 Port Royal Rd.
Springfield, VA 22161

Telephone: (800) 553-6847
Facsimile: (703) 605-6900
E-Mail: orders@ntis.fedworld.gov
Online order: <http://www.ntis.gov/help/ordermethods.asp?loc=7-4-0#online>



SAND2012-1772
Unlimited Release
Printed March 2012

PV Output Smoothing with Energy Storage

Abraham Ellis and David Schoenwald
Photovoltaic and Distributed Systems Integration Department
Multiphysics Simulation Technologies Department
Sandia National Laboratories
P.O. Box 5800
Albuquerque, New Mexico 87185-MS1033

Abstract

This report describes an algorithm, implemented in Matlab/Simulink, designed to reduce the variability of photovoltaic (PV) power output by using a battery. The purpose of the battery is to add power to the PV output (or subtract) to smooth out the high frequency components of the PV power that occur during periods with transient cloud shadows on the PV array. The control system is challenged with the task of reducing short-term PV output variability while avoiding overworking the battery both in terms of capacity and ramp capability. The algorithm proposed by Sandia is purposely very simple to facilitate implementation in a real-time controller. The control structure has two additional inputs to which the battery can respond. For example, the battery could respond to PV variability, load variability or area control error (ACE) or a combination of the three.

ACKNOWLEDGMENTS

This work was funded by the US Department of Energy Solar Energy Technologies Program.

CONTENTS

1. INTRODUCTION	7
2. PV AND BATTERY SYSTEM MODELING	10
3. DESCRIPTION OF SMOOTHING AND SOC TRACKING ALGORITHM	11
4. PERFORMANCE TESTING AND PARAMETER TUNING	12
4.1. Test Cases 1-3.....	13
4.2. Test Cases 4-5.....	14
4.3. Other Tests.....	14
5. CONCLUSIONS.....	25
DISTRIBUTION.....	26

FIGURES

Figure 1. Diagram of PV Smoothing Algorithm.	8
Figure 2. Power plots for Test Case #1.....	15
Figure 3. SOC plots for Test Case #1.	16
Figure 4. Power plots for Test Case #2.....	17
Figure 5. SOC plots for Test Case #2.	18
Figure 6. Power plots for Test Case #3.....	19
Figure 7. SOC plots for Test Case #3.	20
Figure 8. Power plots for Test Case #4.....	21
Figure 9. SOC plots for Test Case #4.	22
Figure 10. Power plots for Test Case #5.....	23
Figure 11. SOC plots for Test Case #5.	24

TABLES

Table 1. Parameters for PV Smoothing Diagram	9
----------------------------------------------------	---

NOMENCLATURE

ACE	Area Control Error
AUX	Auxiliary
BESS	Battery Energy Storage System
DB	Dead Band
DOE	Department of Energy
kW	kilo Watts
kW-h	kilo Watt-hours
LPF	Low Pass Filter
MA	Moving Average
PCS	Power Conditioning System
PV	Photovoltaic
SNL	Sandia National Laboratories
SOC	State of Charge

1. INTRODUCTION

This report describes an algorithm, implemented in Matlab/Simulink, designed to reduce the variability of photovoltaic (PV) power output by using a battery. The purpose of the battery is to add power to the PV output (or subtract) to smooth out the high frequency components of the PV power that occur during periods with transient cloud shadows on the PV array. The control system is challenged with the task of reducing short-term PV output variability while avoiding overworking the battery both in terms of capacity and ramp capability. The algorithm proposed by Sandia is purposely very simple to facilitate implementation in a real-time controller. The control structure has two additional inputs to which the battery can respond. For example, the battery could respond to PV variability, load variability or area control error (ACE) or a combination of the three. The outline of the algorithm appears in Figure 1. The default parameters are defined in Table 1.

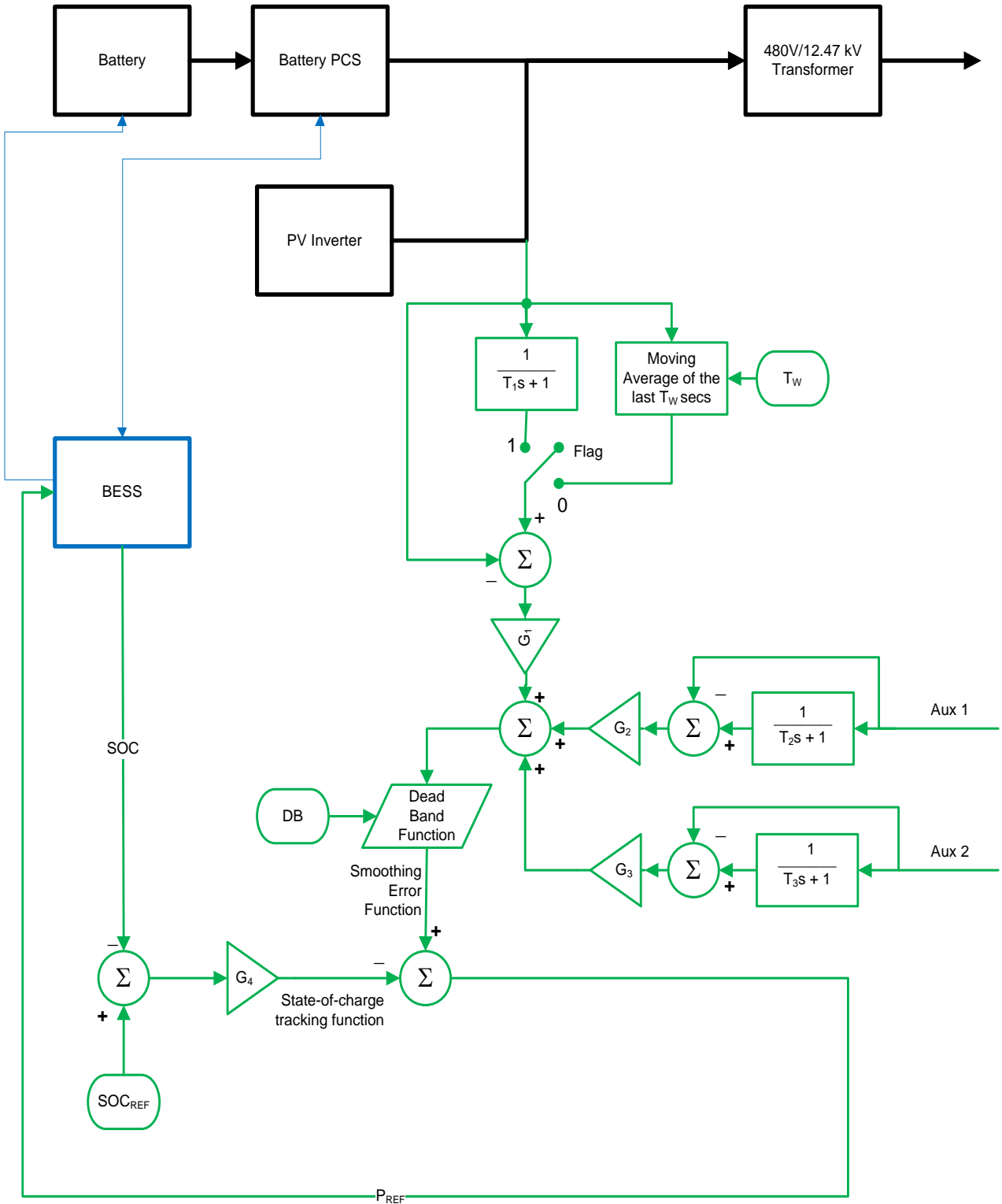


Figure 1. Diagram of PV Smoothing Algorithm.

Table 1. Parameters for PV Smoothing Diagram (*)

Symbol	Name	Units	Default Value
T_w	PV Moving Average Time Window	seconds	3600 (1 hour)
T_1	PV Low Pass Filter Time Constant	seconds	3600 (1 hour)
T_2	AUX1 (load) Low Pass Filter Time Constant	seconds	3600 (1 hour)
T_3	AUX2 (ACE) Low Pass Filter Time Constant	seconds	0
Flag	Switch between LPF and MA	0 or 1, 0=use MA, 1=use LPF	1 (use LPF)
G_1	PV Smoothing Error Gain	unit less	1 (for 100% compensation)
G_2	AUX1 (load) Scaling Factor	unit less	depends on magnitude of AUX1 signal
G_3	AUX2 (ACE) Scaling Factor	unit less	Depends on magnitude of AUX2 signal
G_4	SOC Tracking Gain	unit less	1000
DB	Dead Band Width	kW	+/- 50
SOC_{REF}	Reference State of Charge	unit less (within defined SOC limits)	0.6

(*) These following default parameters were derived assuming a control system sampling rate of 1 second, and for the specific application considered during testing: 500 kW PV, 500 kW power electronics, 1000 kWh battery storage, 0.4 to 0.8 SOC usable range for smoothing.

2. PV AND BATTERY SYSTEM MODELING

The battery itself is modeled as a simple accumulator (integrator). The battery energy storage system (BESS) enforces limits on the range of state of charge (SOC) within which the battery is allowed to operate. These limits are simply represented as saturation limits on the integrator. For this specific application the usable battery SOC range is defined to be 40% to 80% of the battery size (1000 kW-h in this specific case). The SOC limits are expressed as fractions (0.4 and 0.8 in this case). The accumulator (i.e. integrator) has an initial condition that is set to the desired reference SOC value within the allowable range. For this application, a point in the middle of the range was selected which is 0.6 (60% SOC). A time delay was used as a simple way to represent the response time of the BESS and controls in the power electronic devices. The delay is represented by a time constant T_{BESS} . In this specific application, it is assumed that the delay is on the order of 1 sec. The power rating of the power electronics are modeled with a simple power limiter, set to +/- 500 kW, in this particular case. For testing purposes, the PV system was modeled simply as a power injection. Output data from an actual 500 kW PV system was used to test the smoothing algorithm and adjust parameters. Note that, because the algorithm is implemented in Simulink in discrete time using a time step of one second, the power signal going into the integrator is scaled by a factor of 1/3600, which translates power into units of kW-hour. This scaling factor can be easily adjusted both in the model and in the real-time controller.

In summary, the battery energy storage system ultimately commands the battery power level based on a power reference computed by the smoothing algorithm. The BESS takes the desired battery power computed by the smoothing algorithm and delays it by a time constant of T_{BESS} (this is also set by the user and is currently set to 1 sec). Next, a saturation function is applied to limit the requested battery power to no more than +/- the power electronics size (500 kW in this example). Finally, some simple logic makes certain that the requested battery power cannot result in a battery state of charge above SOC_{MAX} or below SOC_{MIN} .

3. DESCRIPTION OF SMOOTHING AND SOC TRACKING ALGORITHM

The smoothed reference signal that the control system is trying to track is either a time moving average (MA) of the PV power, or the PV power processed through a low pass filter (LPF). One of the editable parameters is a flag that determines which of these two smoothing functions is selected. A flag value of 1 implies that the LPF is chosen and a flag value of 0 implies that the MA is chosen. Each of these smoothing functions has a single user editable parameter. The MA function uses the length of the time window, T_w in secs, for its parameter. The default value is 3600 secs (one hour). The LPF function uses the time constant, T_1 also in secs, for its parameter. Again, the default value is 3600 secs. If T_w and T_1 are the same, the two methods create roughly the same smooth reference signal. Figure 1 shows that it is possible to include two auxiliary signals (AUX1 and AUX2) as part of the smoothing function. Both of these can be low pass filtered as well. In general, this control structure allows for representation of a smoothing function of the form $G_1 \times E_1 + G_2 \times E_2 + G_3 \times E_3$, where E_1 is the PV smoothing error signal, E_2 and E_3 are filtered error signals based on AUX1 and AUX2 inputs, and G_1, G_2, G_3 are scaling factors. Neither of the two AUX signals was used in testing of the algorithm, but placeholders exist in the model (and controller) for both. After the smoothing function is obtained, it may be desirable to apply a dead band function to prevent the battery from tracking small excursions from the baseline smoothing function. This dead band width is user settable. For this example, a dead band width of +/- 50 kW was chosen. Table 1 gives the default values for these parameters.

The purpose of the control system is to balance the tasks of tracking the reference SOC value (0.6 in this example) with the desired smoothing function. The state of charge tracking error (difference between the reference SOC and the actual SOC) is multiplied by a proportional gain, G_4 , to produce the state of charge tracking signal. The gain represents how aggressively the battery is returned to the reference state of charge. In a practical application, the gain should be set small enough to allow the smoothing function to take precedence, but large enough to prevent the battery from continuously reaching the defined SOC limits. The SOC tracking signal is then subtracted from the desired smoothing function to determine the reference (requested) battery power for that time step. Once the control system determines the requested battery power this is sent to the BESS which implements it as described above. It should be pointed out that, assuming that the two auxiliary signals are not being used, the two primary parameters of interest are T_w (or T_1 if the LPF is being used) and G_4 . When G_4 is set to 1.0, the battery would be commanded to compensate for 100% of the difference between actual PV output and the smooth reference. A value smaller than 1 could be used if the battery capacity or the power electronics rating is small with respect to the expected PV power error signal. As one increases the time window (or LPF time constant) the smoothed reference signal becomes smoother with slower ramps. The tradeoff is that the battery must make up a larger difference on average for every time step, hence the SOC will have larger excursions from the SOC reference value. Conversely, as G_4 is increased, more emphasis is placed on close tracking of the SOC reference value at the expense of a smoother injected power. The tradeoff between these two parameters allows one to tune the control system to an acceptable balance between the two tasks. Note that the dead band width can also be part of this tuning process.

4. PERFORMANCE TESTING AND PARAMETER TUNING

Various scenarios of parameter values were simulated to illustrate the behavior of the smoothing algorithm and to select appropriate default parameters for the intended application¹. In each case, the PV power output is a one day (86400 second) of measured output from an actual 500 kW PV plant in the southwest US. The selected sample day exhibits significant power output dynamics with some high ramping events, due to cloud shadows on the PV array. Simulations were conducted on 2-5 day PV input signals as well with very similar results, and thus are not included here. In all cases, the sampling rate of the control system is assumed to be 1 second, for simplicity. As discussed in the previous section, system assumptions are as follows:

- 500 kW PV system
- 1000 kWh battery storage
- 500 kW energy storage power electronics converter
- 0.4 to 0.8 SOC usable range for smoothing
- SOC reference value of 0.6

Further, the flag was set to zero meaning that the moving average smoothing algorithm was always used. The low pass filter (LPF) was simulated as well with very similar results. The LPF did result in a slightly smoother smoothing function, but the difference is difficult to discern in these plots, and thus only the MA results are shown in the plots. The PV smoothing gain, G_1 , was set to 1.0 in all test cases. Neither of the auxiliary signals were used during the test, and thus $G_2=G_3=0$ in all cases. For these test cases, the deadband function was disabled ($DB = 0.0$ kW)

In each case two plot charts are presented. The first chart consists of 5 plots of power vs. time where power is in kW and time is in seconds. The first plot is that of PV power. The second plot represents the desired smoothed output. The third plot corresponds to the actual power injected to the grid, which is the sum of PV power plus battery power. The fourth plot represents the difference (in kW) between the actual injected power and the desired smoothed output. The fifth plot corresponds to the power that the battery actually delivers (positive means the battery added to the injected power and negative means the battery used the power to increase its SOC). The difference reflects the battery system response time and SOC limitations, as described in the PV and Battery System Modeling section. The second chart consists of 2 plots of SOC vs. time (in seconds). The first plot is that of the SOC tracking function which is an error tracking signal that is scaled by G_4 and has the units of kW. The second plot corresponds to the actual SOC which is a fraction that should always be between 0.4 and 0.8 (desired value is 0.6 in every case). The results of the test cases discussed below are shown in Figures 2 through 11.

4.1. Test Cases 1-3

Test Case #1 simulates a 15 minute moving average ($TW=900$ seconds) for the smoothing function with a nominal SOC tracking gain ($G_4=1,000$). Figure 2 shows the power plots. Note that the injected power tracks the smoothing function very well with an error not exceeding 28 kW at any time throughout the day. The battery power delivered only briefly exceeds +/- 200 kW. Figure 3 illustrates that the battery SOC remains in a tight range about the reference SOC

¹ The default parameters will be tuned based on local solar resource characteristics, specific control objectives and observed system performance.

barely deviating more than ± 0.02 per unit (2%) from the reference SOC throughout the day. This shows that the battery is able to achieve a 15-minute smoothing average by utilizing only a fraction of its defined usable capacity of 40% (0.4 to 0.8 SOC).

Test Case #2 is identical to Test Case #1 except that the SOC tracking gain is increased by a factor of 10 ($G_4=10,000$). The purpose of this case is to show how tighter tracking of the SOC reference value (i.e. higher G_4 value) affects the tracking of the smoothing function. Figure 4 shows that the smoothing error increases significantly resulting in more high frequency components in the injected power signal. The tradeoff is illustrated in Figure 5 which shows that the battery SOC deviates only about half as much as in Test Case #1. But since the SOC was already well regulated in the first test case, the tradeoff in increased smoothing error is likely not worth the improvement in SOC tracking.

The only change in Test Case #3 is to reduce the SOC tracking gain by a factor of 10 from the nominal value (e.g. $G_4=100$). Figure 6 shows the best smoothing function tracking performance of the first 3 test cases with smoothing errors of no more than ± 4 kW. The price paid is shown in Figure 7 with the battery SOC deviating a little more than in the prior test cases, though not by a significant amount. Test cases 1-3 taken together show that a nominal value of $G_4=1,000$ is quite reasonable with significantly lower values not necessarily stressing the battery that much more while providing improved smoothing performance. Note that for smaller battery sizes, higher deviations from the reference SOC value may not be tolerable, thus the tradeoff between smoothing and SOC tracking is more significant, and thus the value of G_4 should be chosen carefully.

4.2. Test Cases 4-5

These test cases show how the energy storage system time constant (response time of the BESS supervisory control and power electronics controls) affects the performance of the algorithm. With a nominal value of $G_4=1,000$ in each of these cases, the only varied parameter was T_{BESS} with the moving average time window still set to 15 minutes ($T_W=900$ seconds). Test Case #4 sets $T_{\text{BESS}}=1$ second. Compared to Test Case #1, the addition of a nominal BESS time delay shows little change in the magnitude of the smoothing error signal as shown in Figure 8. But there is significantly more time variation in the smoothing error (i.e. more high frequency components). This is due to the time delay between when the desired battery power signal is determined and when the actual battery power signal is applied to the injected power. A BESS time delay of one second does not have much of an effect on the smoothing performance, and does not significantly affect SOC tracking performance as shown in Figure 9.

Test Case #5 illustrates the performance of the algorithm when T_{BESS} is increased significantly, in this case to $T_{\text{BESS}}=30$ seconds. Figure 10 shows that not only has the smoothing error increased in magnitude (more than double) but the high frequency components are substantially more evident as seen in the injected power plot. Figure 11 shows that the SOC tracking is about the same as in Test Case #4.

4.3. Other Tests

Further testing was conducted with longer average time window, as high as 2 hours. For these tests, SOC remains well within the 0.4 to 0.8 limits, and the required battery power rarely challenges the rating of the power electronics. Of course, longer time windows improve the smoothing performance at the expense of increasing the battery usage and higher charge/discharge rates. In the interest of brevity, however, further results are not shown. The use of the low pass filter instead of the moving average showed a small improvement in smoothing performance with minimal additional battery usage. The simulation of all these tests resulted in the nominal parameter values chosen in Table 1 which produced desired overall performance.

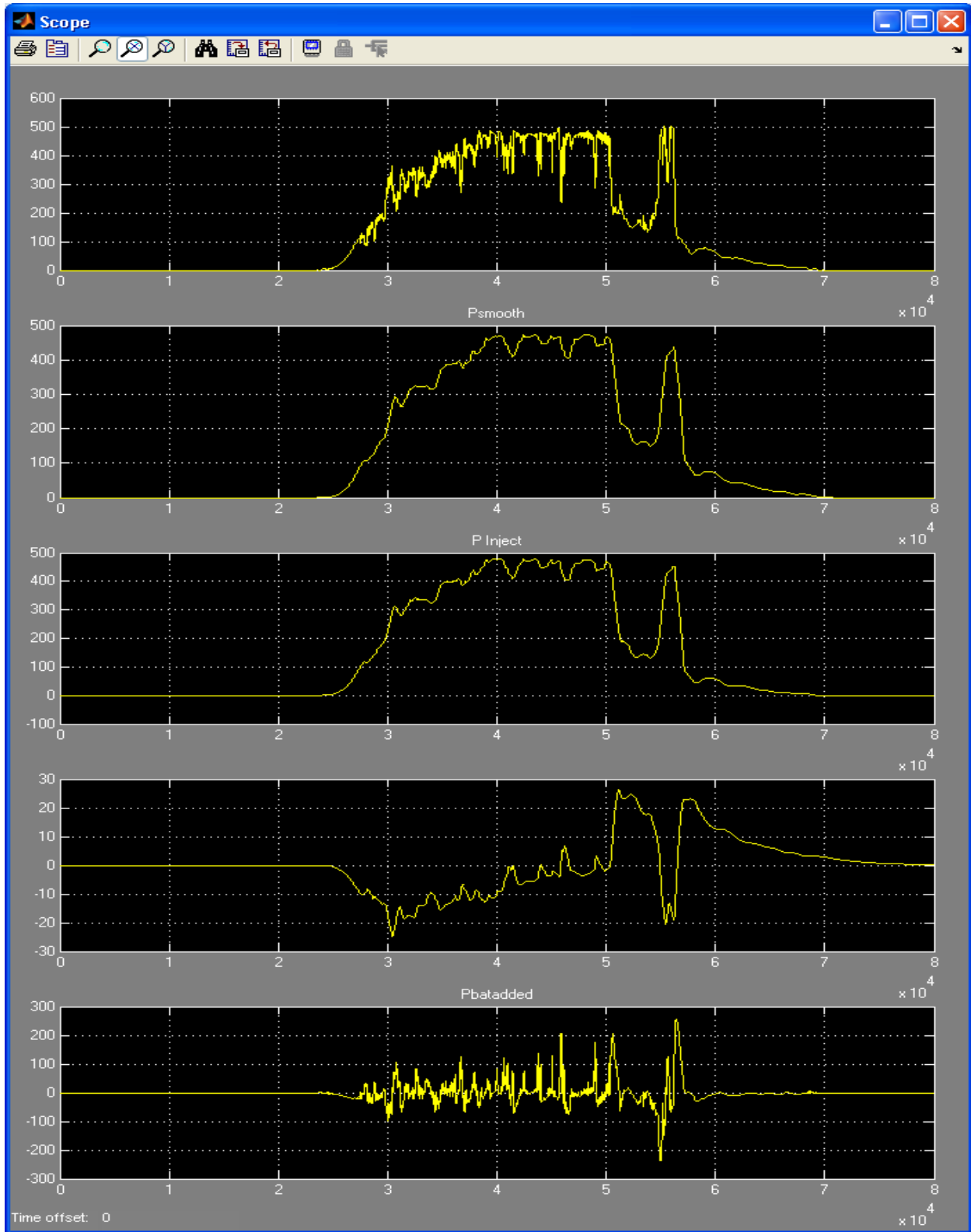


Figure 2. Power plots for Test Case #1.

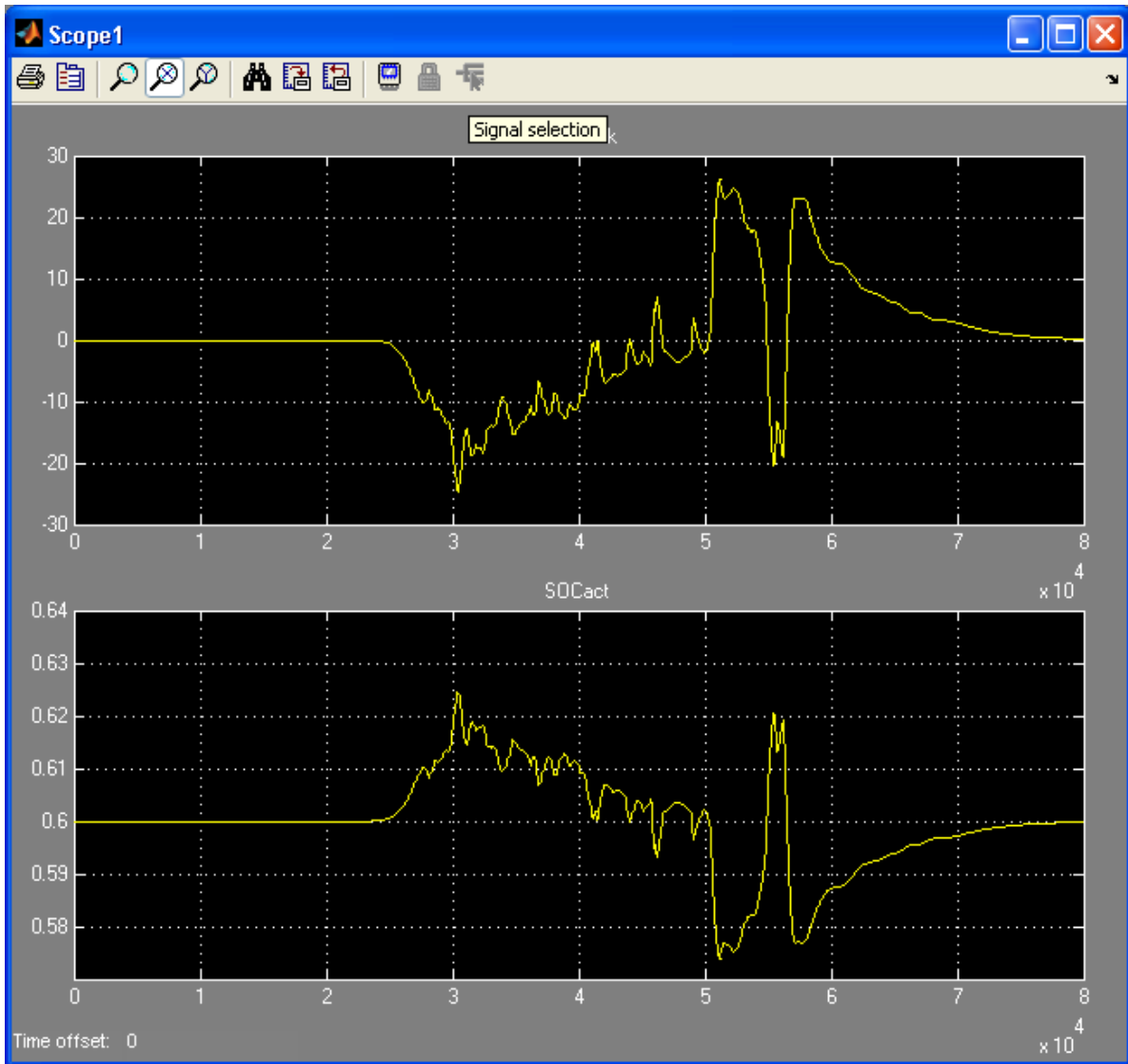


Figure 3. SOC plots for Test Case #1.

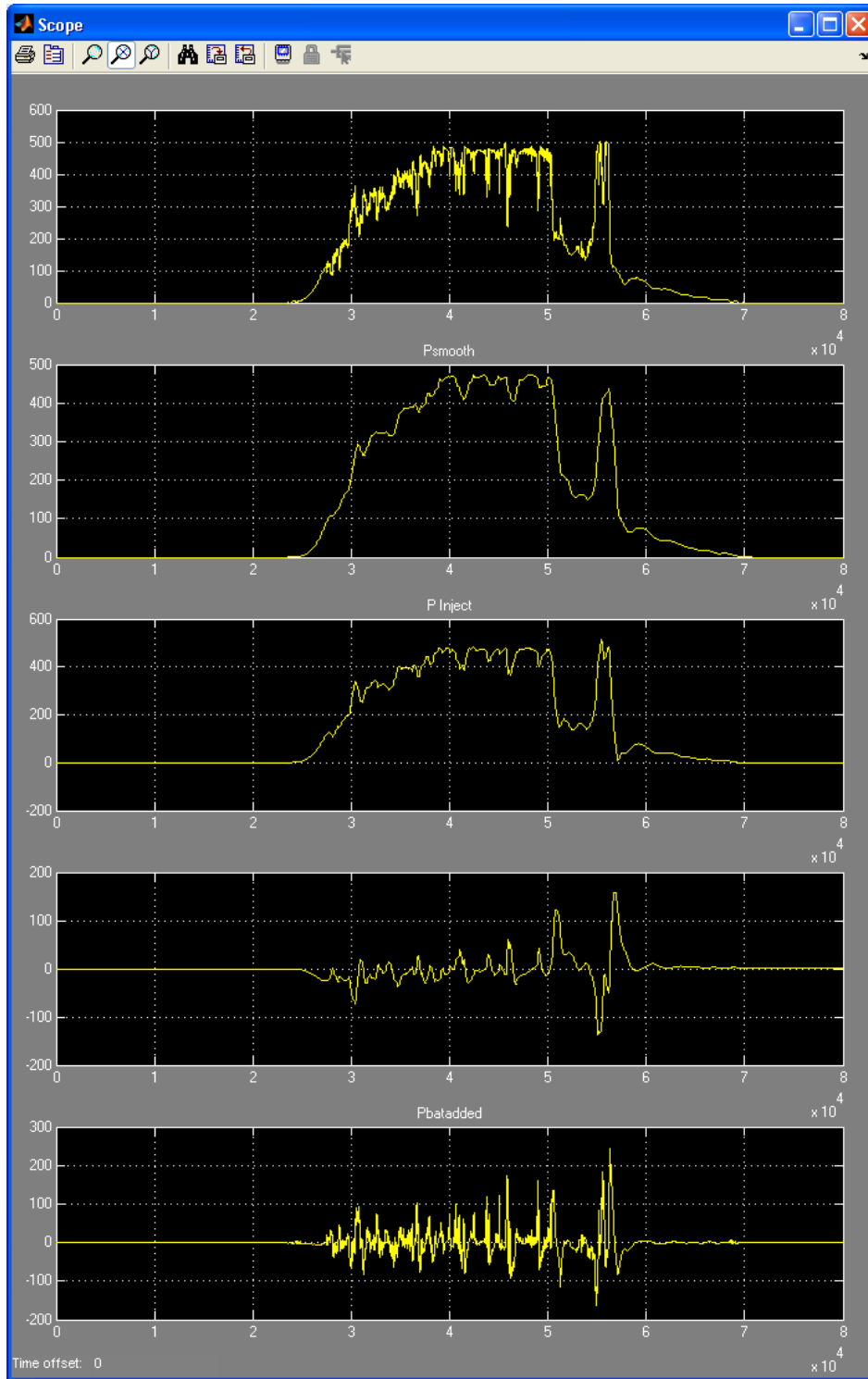


Figure 4. Power plots for Test Case #2.

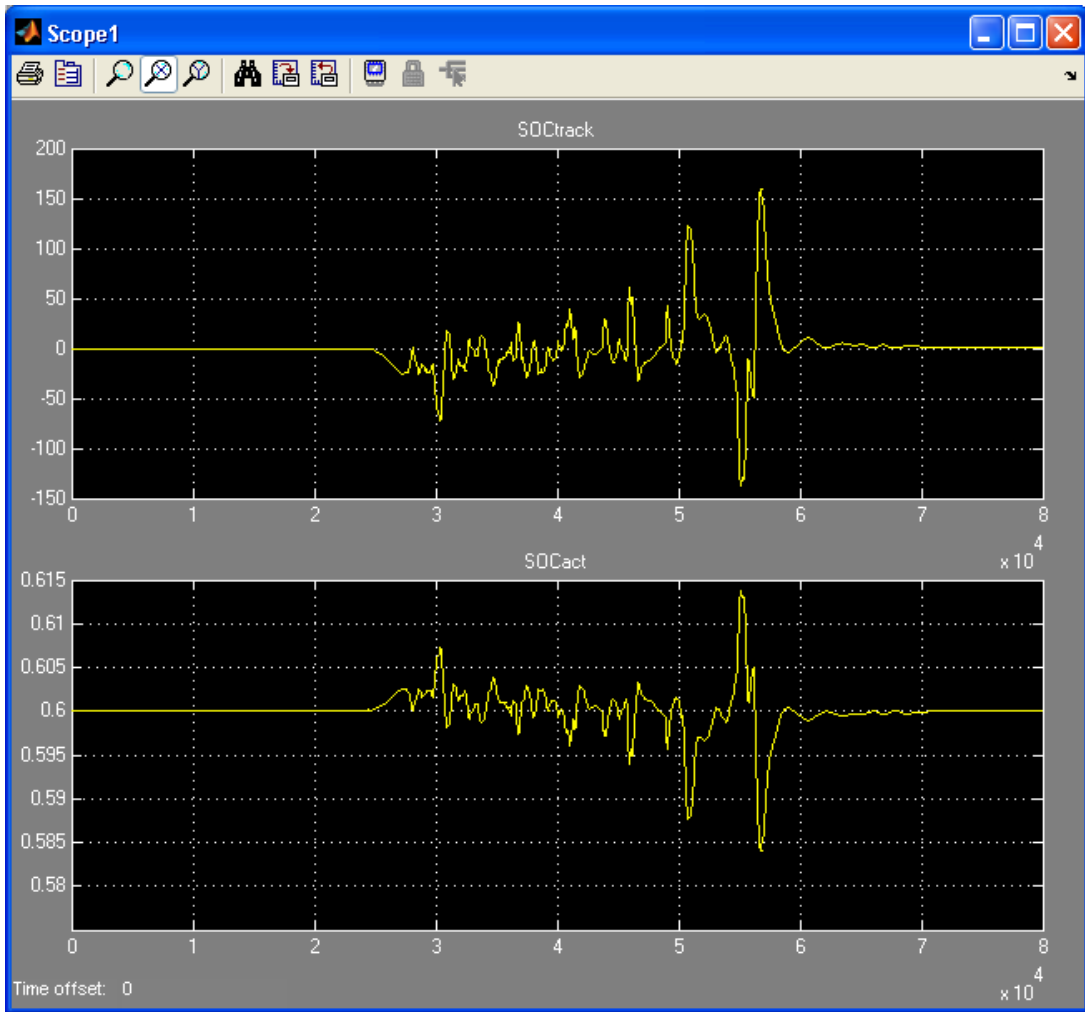


Figure 5. SOC plots for Test Case #2.

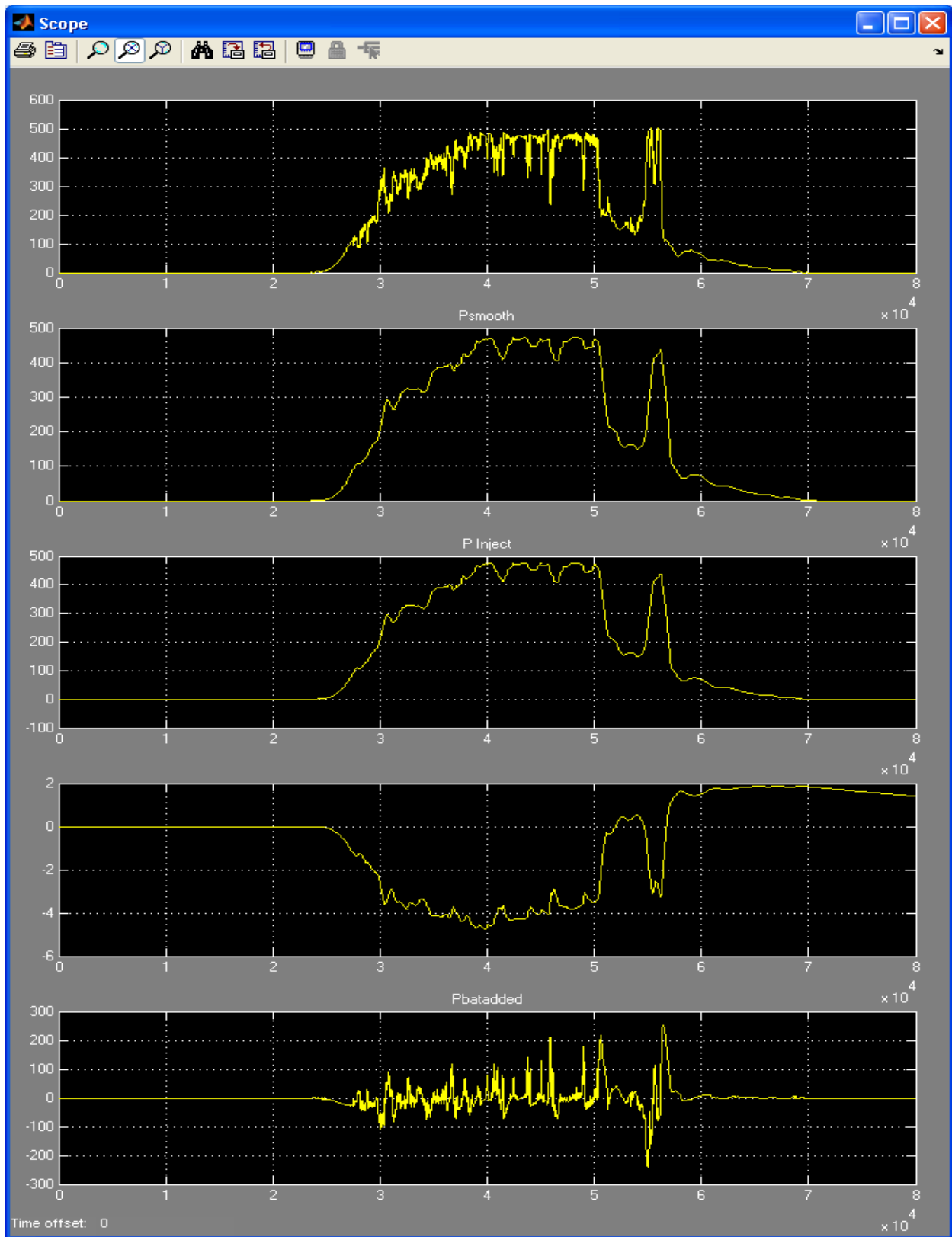


Figure 6. Power plots for Test Case #3.

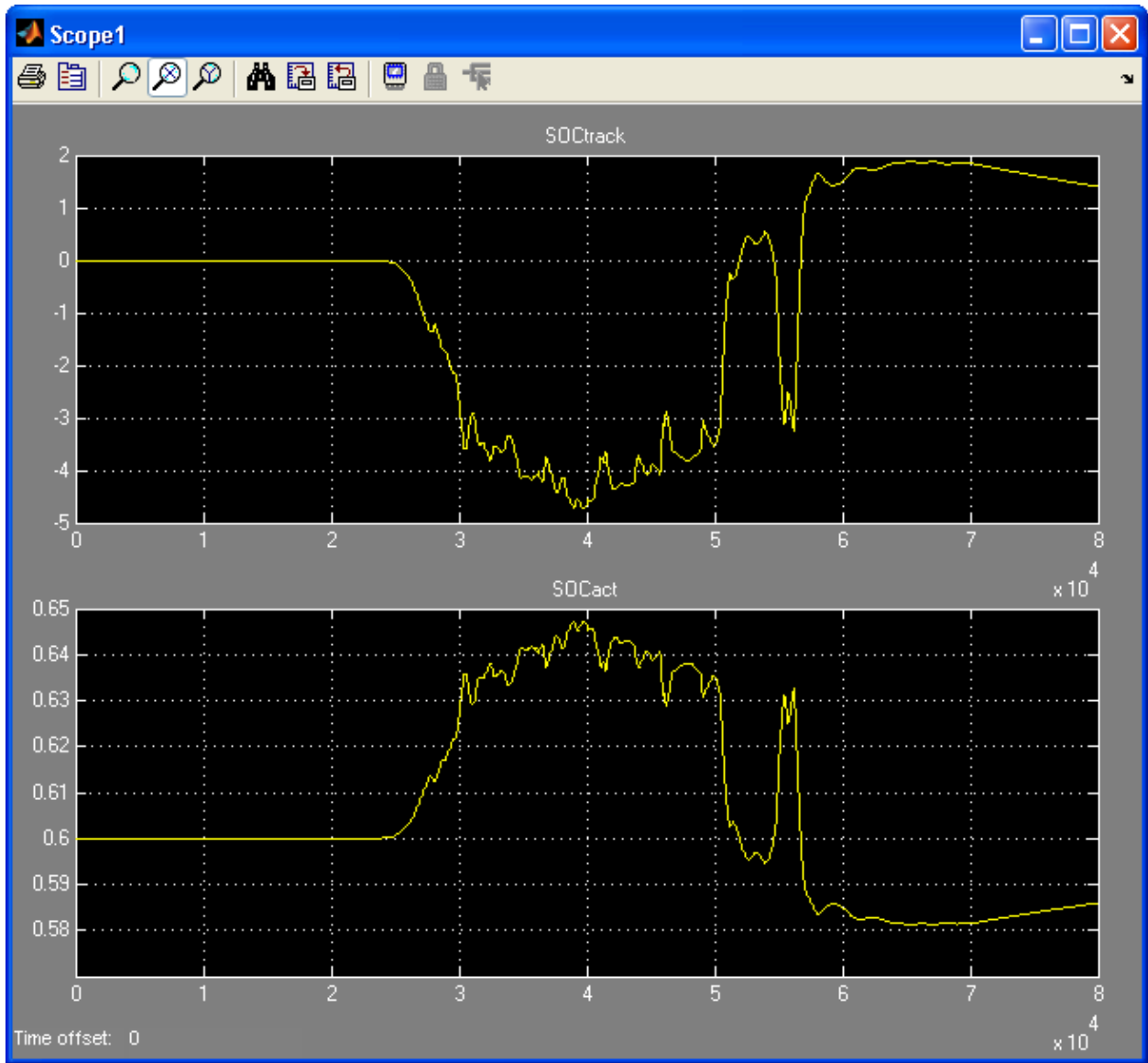


Figure 7. SOC plots for Test Case #3.

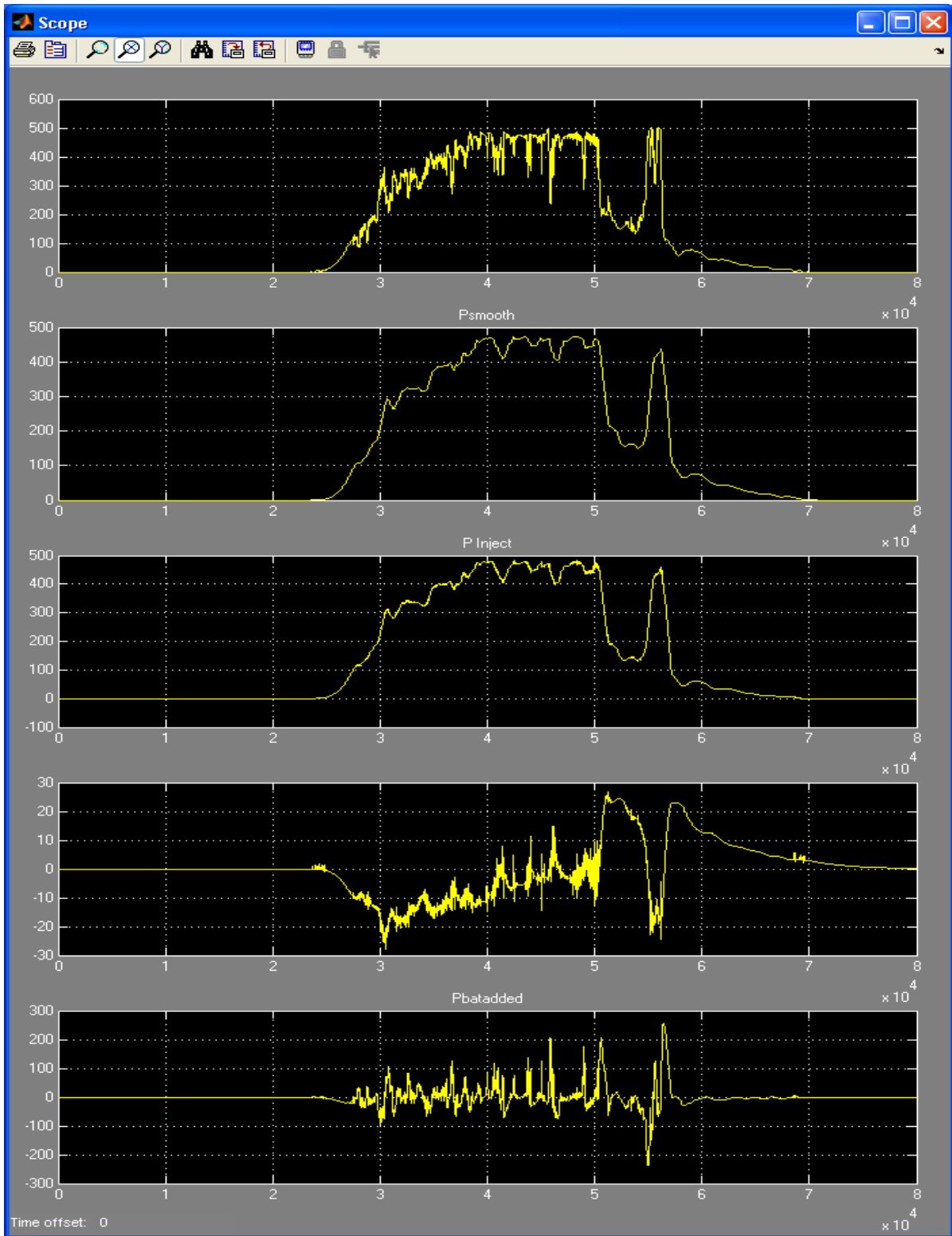


Figure 8. Power plots for Test Case #4.

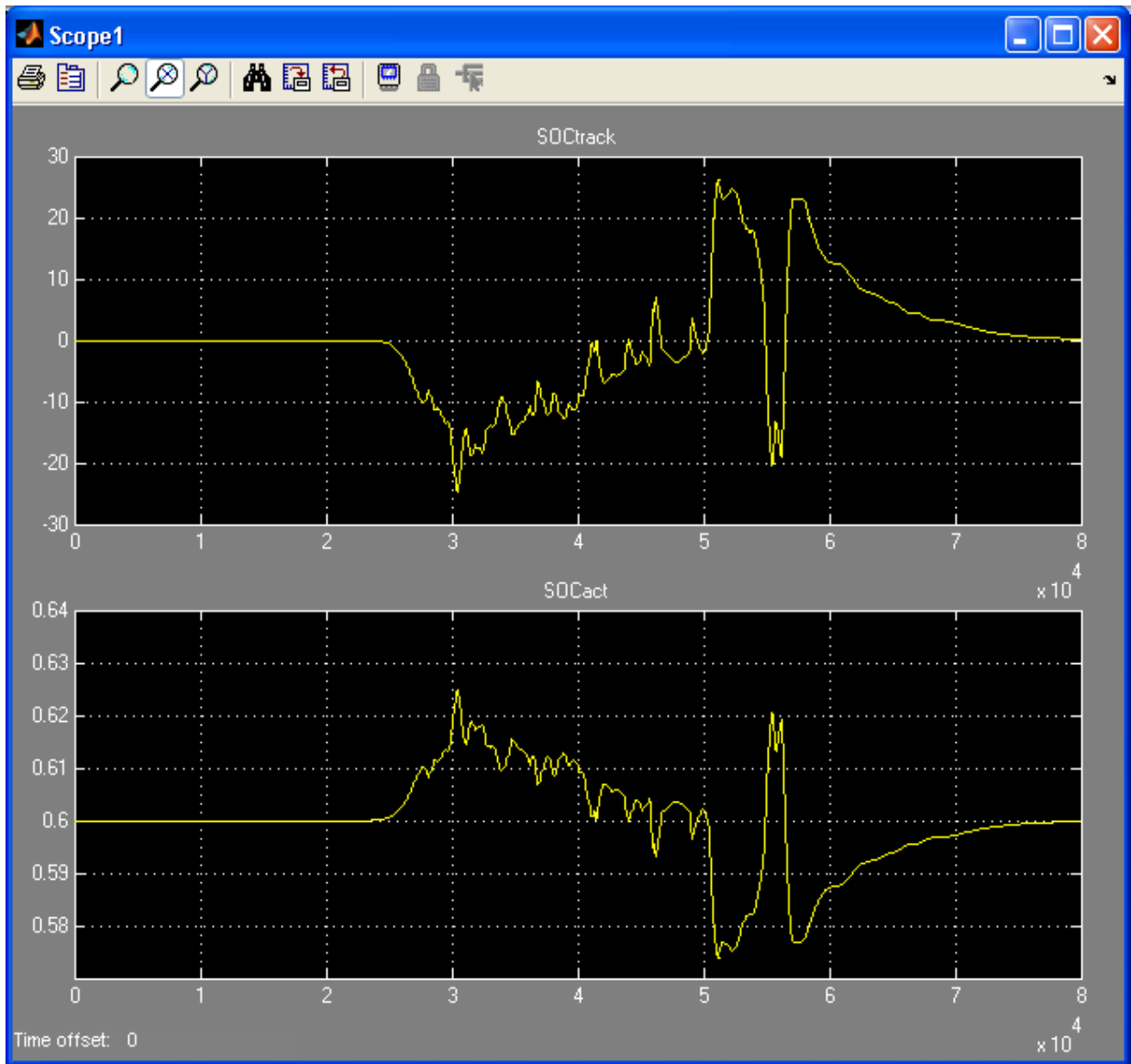


Figure 9. SOC plots for Test Case #4.

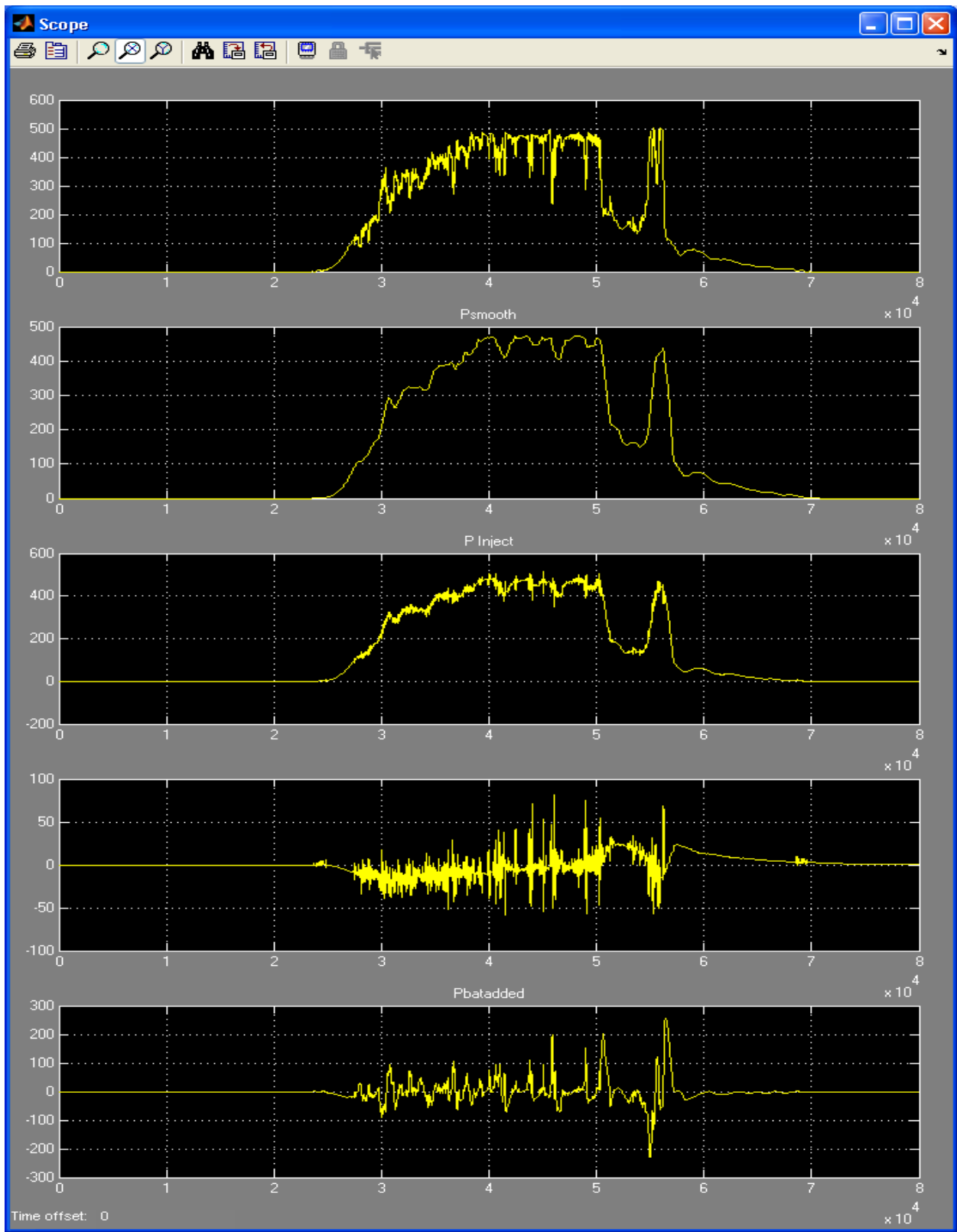


Figure 10. Power plots for Test Case #5.

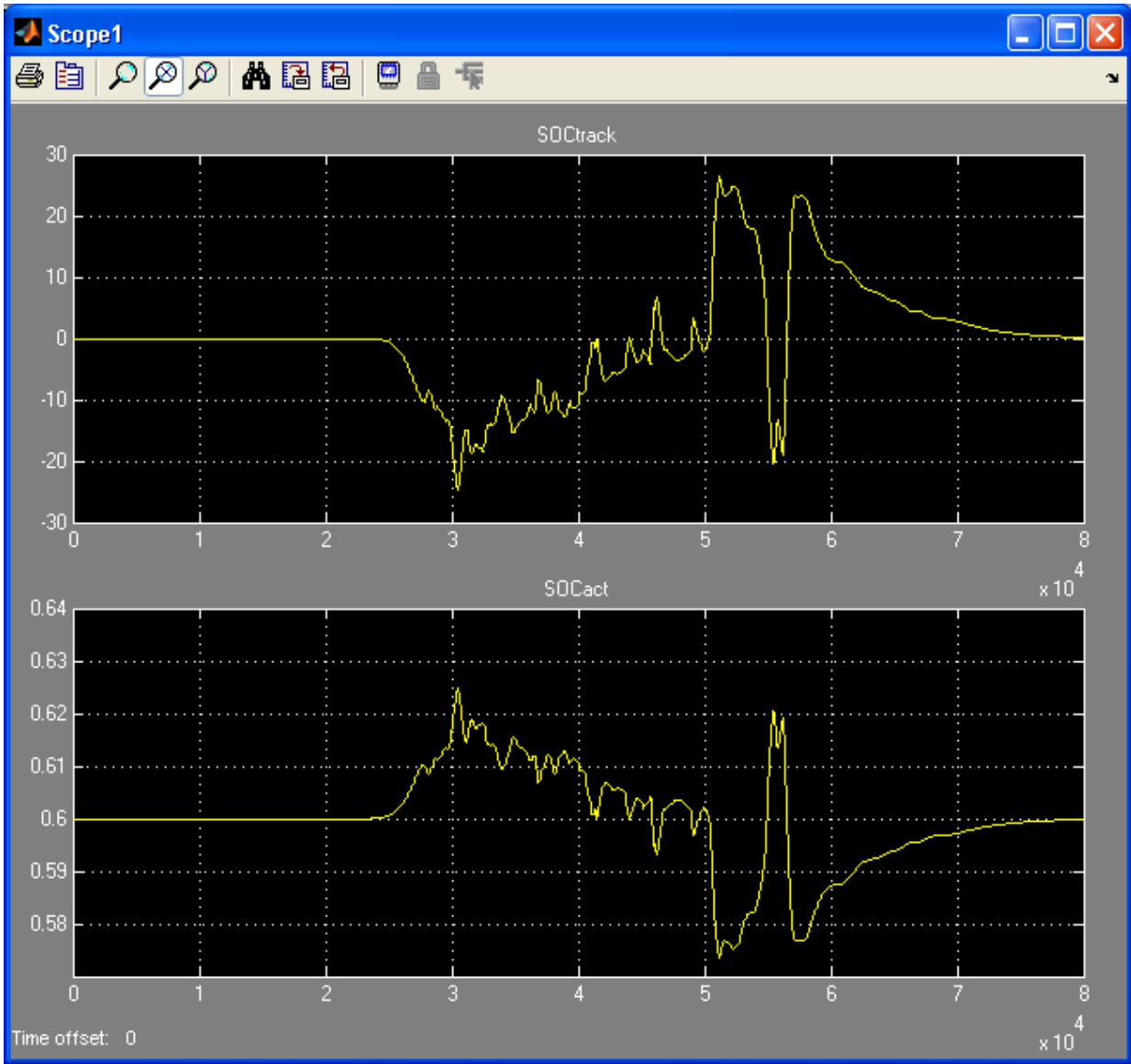


Figure 11. SOC plots for Test Case #5.

5. CONCLUSIONS

This report describes an algorithm designed to reduce the variability of photovoltaic (PV) power output by using a battery. The algorithm presented was designed to be implemented in real time thus it does not contain a significant amount of complexity. The system parameters (battery capacity, rating of converters, and PV system rating) were assumed to be fixed. This exercise did not attempt to optimize the size of the energy storage system. Different battery parameter values would likely result in a change in the nominal parameter values needed to produce continued satisfactory overall performance.

A very simple model was used to represent the battery system. The effect of temperature, charge/discharge rate, efficiency and equalization charging were not considered. Such refinement could be added to the model, but their impact on the overall controller performance is not expected to be very significant. In this implementation, only MA and LPF smoothing options were evaluated. More sophisticated options with more general filtering capabilities are certainly possible, but were not evaluated. In addition, a few changes to the control system could be made to improve the robustness of the control system to battery parameters and time delays. The dead band function helps, but other changes could include variable gains that adapt depending on the magnitudes of the error signals or incorporating prediction functions to correct for time delays naturally introduced by the MA and LPF functions. Finally, more testing can be done to demonstrate the addition of the two auxiliary signals to show their effects on the algorithm's performance. Much of this experimentation is planned as part of the field demonstration.

DISTRIBUTION

1	MS0614	Summer R. Ferreira	02546
1	MS0614	Thomas D. Hund	02547
1	MS0721	Marjorie L. Tatro	06100
1	MS0734	Stanley Atcitty	06121
1	MS0734	Anthony Martino	06124
1	MS1033	Abraham Ellis	06112
1	MS1033	Charles J. Hanley	06112
1	MS1033	Clifford W. Hansen	06112
1	MS1033	Jimmy Quiroz	06112
1	MS1033	Joshua S. Stein	06112
1	MS1082	Anthony L. Lentine	01727
1	MS1104	Rush D. Robinett III	06110
1	MS1104	Juan J. Torres	06120
1	MS1108	Daniel R. Borneo	06111
1	MS1108	Ray E. Finley	06111
1	MS1108	Benjamin L. Schenkman	06111
1	MS1124	David G. Wilson	06122
1	MS1137	Mark E. Ralph	06925
1	MS1140	Raymond H. Byrne	06113
1	MS1140	Ross Guttromson	06113
1	MS1140	Georgianne Huff	06113
1	MS1140	David M. Rose	06113
1	MS1140	David A. Schoenwald	06113
1	MS1140	Cesar A. Silva Monroy	06113
1	MS1152	Steven F. Glover	01654
1	MS1152	Jason C. Neely	01654
1	MS1318	Robert J. Hoekstra	01426
1	MS0899	RIM-Reports Management	09532 (electronic copy)



Sandia National Laboratories